American Journal of Biochemistry and Biotechnology

Research Notes

Nuciferine Attenuates Cigarette Smoke-Induced Senescence in HepG-2 Cells via the miR-217/SIRT1/Nrf2 Pathway

Yun-Hong Zhao, Yi-Meng Ge, Wei-Jia Xu, Xue-Qing Wang, Feng Guan and Jian Ge

College of Life Sciences, China Jiliang University, Hangzhou, China

Article history
Received: 15-02-2025
Revised: 21-05-2025
Accepted: 26-05-2025

Corresponding Author:
Jian Ge
College of Life Sciences, China Jiliang University, Hangzhou, China
Email: gejian@cjlu.edu.cn

Abstract: The lotus leaf, widely used in both medicine and cuisine, contains bioactive compounds with therapeutic potential. Nuciferine (NF), an active constituent of significant importance, is extracted from the lotus leaf. The present study sought to uncover the molecular pathways through which Nuciferine (NF) mitigates cellular senescence triggered by Cigarette Smoke Components (CSCs) in HepG-2 cells, employing an experimental model where NF was administered to CSC-induced HepG-2 cells.Reverse transcription polymerase chain reaction (RT-PCR) was employed to assess the expression of aging-related genes within HepG-2 cells The expression profiles of endogenous miRNAs were analyzed, while the regulatory relationship between miR-217-5p and SIRT1 was examined through Dual Luciferase Reporter Gene Assay (DLRG). Nuciferine treatment significantly increased antioxidant enzyme levels (SOD and GSH-Px) while reducing malondialdehyde (MDA) levels compared to CSC-treated cells ($P<0.05$). Additionally, SIRT1, Nrf2, and FOXO1 expression levels were significantly upregulated in the NF-treated group ($P<0.05$). The targeting association between miR-217-5p and SIRT1 mRNA was further substantiated using the DLRG approach. Mechanistic investigations revealed that NF counteracts CSC-triggered senescence in HepG-2 cells through miR-217-5p-mediated regulation of its downstream targets, leading to subsequent activation of the SIRT1/Nrf2 cascade. These findings position Nuciferine as a promising dietary compound with potential anti-aging properties.

Keywords: Nuciferine, Cigarette Smoke Components, SIRT1, miR-217

Introduction

Smoking is strongly linked to tuberculosis (TB). It impairs lung function and weakens immunity, increasing susceptibility to TB infection. TB remains a major global health challenge, particularly in developing countries (Ahmad *et al.*, 2024). Cigarette smoke exposure contributes to hepatic oxidative stress and cellular senescence, posing significant risks for Non-Alcoholic Fatty Liver Disease (NAFLD) development (Enc *et al.*, 2020; Yang *et al.*, 2022). As the primary metabolic organ, the liver is particularly vulnerable to xenobiotic-induced damage, with cigarette-derived compounds known to disrupt redox homeostasis and mitochondrial function (Granata *et al.*, 2023). These pathological changes share molecular hallmarks with aging processes, particularly through oxidative stress-mediated cellular senescence (Kaur *et al.*, 2021; von Zglinicki, 2024).

The miR-217/SIRT1 axis has emerged as a critical regulator of cellular senescence (Zhang *et al.*, 2025). miR-217 promotes oxidative stress and accelerates senescence by targeting SIRT1, a NAD+-dependent deacetylase essential for maintaining redox balance (Wang *et al.*, 2021; Menghini *et al.*, 2009). This regulatory network intersects with the Nrf2 pathway, forming an integrated defense system against oxidative damage (Yang *et al.*, 2025). However, the specific mechanisms by which this pathway mediates cigarette smoke-induced hepatocyte senescence remain poorly understood.

Medicinal food homology substances offer promising interventions for oxidative stress-related pathologies (Dong *et al.*, 2024; Liu *et al.*, 2025). The study indicates that the ethanol extract from Catharanthus roseus leaves exhibits remarkable antioxidant activity, with an IC50 value as low as 3.3 ppm, demonstrating its potent ability to counteract oxidative stress. The extract is rich in triterpenoid compounds such as α-amyrin and lup-20(29)-en-3-ol, which are identified as the primary contributors to its antioxidant potential (Zulfikar *et al.*, 2024). Active compounds in tung leaf extract exhibit significant antioxidant and anti-inflammatory potential, effectively reducing inflammation by suppressing TNF-α levels in a dose-dependent manner (Zahara *et al.*, 2024).

The Nuciferine, in lotus leaves are natural phytochemicals, and studies have shown that phytochemicals can exert multiple antioxidant effects through activation of the Nrf2 pathway. (Wu *et al.*, 2022). Recent evidence demonstrates its hepatoprotective effects against ethanol-induced damage via miR-144/Nrf2 modulation (Fang *et al.*, 2024), suggesting potential cross-talk with related microRNA pathways. Nevertheless, its impact on miR-217-mediated hepatocyte senescence has not been investigated.

This study investigates the cytoprotective mechanism of Nuciferine against cigarette smoke component-induced hepatocyte senescence, focusing on the miR-217/SIRT1/Nrf2/FOXO1 axis. By systematically elucidating these molecular interactions, this study advances the understanding of the critical signaling pathways underlying cigarette smoke extract-induced hepatocyte senescence, provides robust experimental evidence supporting Nuciferine's anti-aging efficacy, and lays the groundwork for developing novel anti-hepatic senescence therapeutics based on the medicinal food homology principle.

Materials and Methods

Instruments and Materials

Nuciferine (purity >98%) was obtained from Med Chem Express Co. (Shanghai, China). The HepG-2 cell line was acquired from the American Type Culture Collection (ATCC, USA). Cell maintenance was performed in DMEM medium supplemented with 10% fetal bovine serum (both from Nanjing Kaiji Biology, China), under standard culture conditions (37°C, 5% CO2). Commercial assay kits for SOD, MDA and GSH-Px detection, along with Trizol® Plus RNA Purification Kit and Transcriptor First Strand cDNA Synthesis Kit, were sourced from Thermo Fisher Scientific (Waltham, MA, USA). The dual-luciferase reporter assay system was procured from Promega Corporation (Madison, WI, USA).

The experimental investigations were conducted utilizing the Spectra Max 190 full-wavelength microplate reader (Molecular Devices, USA) for absorbance measurements, along with laboratory-prepared filter cigarettes manufactured from single-grade tobacco leaves. Particle size characterization was performed using the Zetasizer Nano ZS90 system (Malvern Panalytical, UK), while cellular imaging was accomplished with the OLYMPUS BX60 fluorescence microscope (Olympus, Japan). Ultrastructural analyses employed a Hitachi transmission electron microscope (Hitachi High-Tech, Japan), and gene expression profiling was carried out on the CFX384 real-time PCR platform (Bio-Rad, USA) using PowerUp™ SYBR™ Green Master Mix (Applied Biosystems，USA).

Preparation of Cigarette Smoke Components

As delineated in a prior investigation (Ge *et al.*, 2022), a custom-built smoking generation and collection apparatus was employed to prepare a cigarette extract. The flow rate of the extract and the combustion duration for each cigarette were meticulously regulated, with each cigarette being burned for a precise period of 4 minutes. A volume of 100 ml of sterile saline was circulated through 16 cigarettes to obtain the extract. For convenience in subsequent experiments, the cigarette extract diluted 16 times from the original solution was labeled as 100%. The apparatus for the preparation of smoking extract components is depicted in Figure 1.

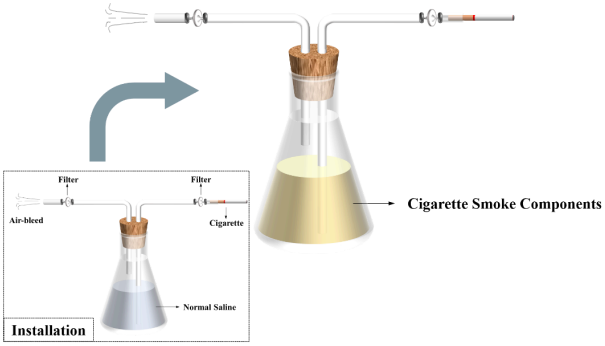

Fig. 1: CSCs preparation device. The cigarette was mounted onto a smoke generator, with the smoke being directed into a screw-capped bottle holding 100 mL of sterile saline solution

Cell Culture and Cell Biability Assays

HepG-2 cells were propagated in DMEM supplemented with 10% fetal bovine serum and 1% penicillin-streptomycin, maintained at 37°C in a 5% CO_2 atmosphere. The medium was replenished every two days, with exponentially growing cells being harvested for experimental use. Cell suspensions were prepared at a density of 1×10^5 cells/mL and distributed into 96-well plates (100 µL per well). Experimental groups consisted of: blank (medium only), control (cells with medium), D-galactose (37.5, 75, 150, 300 mM), and CSCs (6.25, 12.5, 25, 50, and 100%), all conditions being replicated six times. After 48 hours of treatment, the medium was aspirated and replaced with 10 µL CCK-8 reagent per well for a 2-hour incubation. Absorbance measurements at 450 nm enabled viability calculation using the standard formula: [(An experimental group - A blank group)/(A control group - A blank group)] ×100%.

SA-β-Gal Staining

HepG-2 cell suspension was seeded into 24-well plates (5×10^4 cells/mL, 500 µL/well). Following 24 h culture, the model group was treated with 500 µL of medium supplemented with 25% CSCs and 75 mM D-

galactose, whereas the control group retained standard medium. In the NF intervention group, 500 μL of medium with 50 μM NF was administered. Triplicate wells were prepared for each condition. After 24 h, the medium was aspirated, followed by a single PBS wash. Cells were then fixed with 500 μL β-galactosidase staining fixative (15 min, RT) and rinsed thrice with PBS (3 min/wash). Subsequently, 1 mL of staining solution was added per well, and samples were incubated overnight at 37°C prior to microscopic imaging.

Determination of Oxidative Stress Indicators in HepG-2 Cells

HepG-2 cells were plated in 6-well plates (10^5 cells/mL) and maintained for 24 h. Subsequently, the medium was refreshed with 2 mL of fresh medium containing 25% CSCs combined with 50 μM NF, followed by a 48 h incubation period. The cells were then harvested, and SOD/GSH-Px activities along with MDA levels were quantified using commercial assay kits. Control groups included CSC-treated cells and untreated cells.

qRT-PCR

Thawed cell samples were lysed in 1 mL TRIzol® Reagent, followed by RNA extraction and purification using an RNA purification kit. RNA concentration, purity, and integrity were assessed, followed by normalization to equivalent RNA quantities. The qPCR primers were designed utilizing Primer Premier 6.0 and Beacon Designer 7.8 software packages, with detailed sequences provided in Tables 1 and 2. Gene expression was quantified by real-time PCR in triplicate, calculate the relative expression levels of each gene according to formula $2^{(Ct\ reference\ gene\ -\ Ct\ target\ gene)}$.

Table 1: Real-Time PCR Primers and Conditions

Gene	Genbank Accession	Primer Sequences (5' to 3')	Size (bp)	Temperature (°C) with buffer conditions
Human GAPDH	NM_002046.5	CCATGACAACTTTGGTATCGTGGAA	107	60
		GGCCATCACGCCACAGTTTC		
Human FOXO	NM_002015.3	GGTATGAACCGCCTGACCCAA	171	60
		AATGAACATGCCATCCAAGTCACT		
Human NRF2	NM_001145412.2	CAGCCCAGCACATCCAGTCAG	161	60
		CTGAAACGTAGCCGAAGAAACCTCA		
Human SIRT1	NM_001142498.1	GGAGGAGCTGGATTTGGGACTGAT	143	60
		GGTGGAACAATTCCTGTACCTGCACA		

Table 2: Real-Time PCR Amplification System and Conditions

	20 μlSystem
SDW	8.0 μl
Power SYBR® Green Master Mix	10.0 μl
Forward Primer (10 μM)	0.5 μl
Reverse Primer (10 μM)	0.5 μl
cDNA	1.0 μl

Reaction conditions: 95°C for 1 min; 40 cycles (95°C, 15 sec, 63°C, 25 sec, with fluorescence collection); Melting curve from 55 to 95°C

MiRNA Genome Sequencing

Cell lysates were prepared using 300 μL of Binding Buffer with vigorous vortexing, followed by centrifugation at 12,000×g for 10 min. The resulting supernatant was carefully pipetted into a Spin Cartridge assembly. For RNA purification, the flow-through was combined with 70% ethanol, thoroughly mixed, and applied to a fresh Spin Cartridge. Subsequent centrifugation (12,000×g, 1 min) enabled flow-through disposal. The column then underwent three sequential washes with 500 μL Wash Buffer (12,000×g, 1 min each), followed by a drying spin (12,000×g, 5 min). RNA was ultimately eluted with 50 μL RNase-Free ddH2O after a 2 min incubation period. MicroRNA quality control was performed through dual assessment by spectrophotometric measurement and electrophoretic analysis, with subsequent quantity normalization. For qPCR analysis, primer sequences (Tables 3-4) were computationally designed using Primer Premier 6.0 and Beacon Designer 7.8 platforms. Quantitative real-time PCR was conducted in technical triplicates, with relative gene expression determined via the comparative Ct method ($2^{(Ct\ reference\ gene\ -\ Ct\ target\ gene)}$).

Table 3: Forward Primer for Real-Time PCR and Conditions

Gene	Forward Primer and Universal Primer (5' to 3')	Temperature (°C) with buffer conditions
hsa-miR-217-5p-F	CGCGTACTGCATCAGGAACTG	60
Ext-F	CACCGGGTGTAAATCAGCTTG	60
micro-R	AGTGCAGGGTCCGAGGTATT	60

Table 4: Real-Time PCR Amplification System and Conditions

	20 μl System
SDW	8.0 μl
Power SYBR® Green Master Mix	10.0 μl
Forward Primer (10 μM)	0.5 μl
micro-R (10 μM)	0.5 μl
cDNA	1.0 μl

Reaction conditions: 95°C for 1 min; 40 cycles (95°C, 15 sec, 60°C, 25 sec, with fluorescence collection); Melting curve from 55 to 95°C

Dual Luciferase Assay

According to the dual-luciferase reporter assay method with slight modifications, prior to transfection experiments, 293T cells exhibiting robust logarithmic-phase growth were carefully plated in 24-well culture plates. Transfection procedures were subsequently initiated using Lipofectamine^{TM} 3000 when visual inspection confirmed cellular coverage approaching 60% of the culture surface area. Before transfection, fresh culture medium was replaced. miRNA-217-5p mimic was prepared at a concentration of 20 pmol/well, and 500 ng/well of recombinant plasmid pmirGLO-SIRT1-WT or pmirGLO-SIRT1-MUT was added. Freshly prepared culture medium in 24-well plates was maintained under standard culture conditions (37°C, 5% CO2) for an 8-hour equilibration period. Following a 48-hour incubation, two PBS washes were performed per well prior to cell lysis using 250 μL of 1×PLB buffer at ambient temperature. For luminescence measurement, 100 μL LARII reagent was dispensed into opaque 96-well plates, followed by addition of 20 μL lysate. Immediate luminescence readings were acquired before rapid introduction of 100 μL Stop & Glo substrate (<10 sec), with subsequent measurements recorded. The following commercial reagents were employed: Lipofectamine^{TM} 3000 transfection reagent (Thermo Fisher Scientific, China), TRIzol® Plus RNA purification kit and Transcriptor first-strand cDNA synthesis kit (Thermo Fisher Scientific, USA), along with the dual-luciferase reporter assay system (Promega Corporation, Madison, WI, USA).

Statistical Analysis

Experimental data are presented as mean ± SD values. Statistical analyses were performed using one-way ANOVA with SPSS software (version 20.0). Significance thresholds were defined as follows: $P>0.05$ (ns, non-significant), $P<0.05$ (*, statistically significant), and $P < 0.01$ (**, highly significant).

Results

Major Components of CSCs

The gas chromatography–mass spectrometry (GC-MS) analysis of CSCs identified 100 chemical constituents, comprising 14 neutral components, 44 acidic components, and 40 basic components. The mass spectra of these components are presented in Figure 2. The mass spectra of these components were cross-referenced against both Willey and NISTO2 spectral libraries. Glyceryl triacetate emerged as the predominant constituent (75.92%) in the neutral fraction, while 2,4-(1,1-dimethylethyl)phenol and nicotine constituted the major components in the acidic (17.63%) and basic (39.29%) fractions, respectively.

Cytotoxicity-Based Safety Concentration Screening

CCK-8 assay data in Fig. 3 defined the non-toxic concentration windows for all tested compounds: Nuciferine preserved normal cellular functions at 5–50 μM, D-galactose demonstrated equivalent biosafety at 5–150 mM, and CSCs manifested comparable non-toxicity at 6.25–25%. Therefore, the final concentrations selected for drug intervention and model establishment were: Nuciferine, 50 μM; D-galactose, 75 mM; and CSCs, 25%.

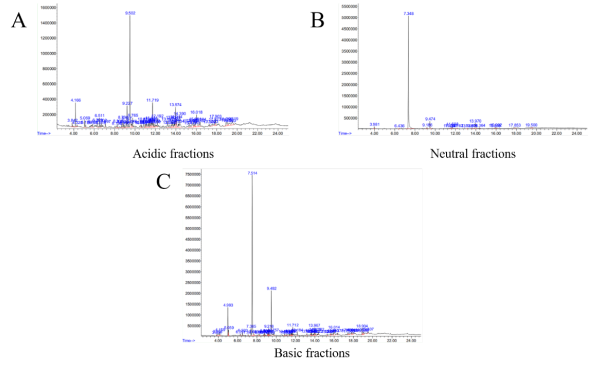

Fig. 2: Mass spectrometric analysis of CSC fractions: (A) Acidic fraction, (B) Neutral fraction, (C) Basic fraction

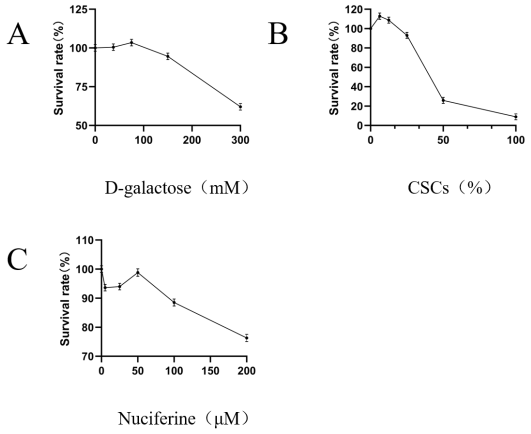

Fig. 3: CCK-8 assay results in HepG2 cells: (A) D-galactose, (B) Cigarette smoke condensates (CSCs), (C) Nuciferine

NF Significantly Attenuated CSCs-Induced Senescence in HepG-2 Cells

Cellular senescence models were established in HepG2 cells using either D-galactose or CSCs as senescence inducers, with subsequent senescence assessment performed via SA-β-gal staining at pH 6.0, where senescent cells exhibit elevated β-galactosidase activity that catalyzes substrate conversion to produce characteristic dark blue precipitates visible under light microscopy. As illustrated in Fig. 4, comparative analysis revealed successful senescence induction in both D-galactose-treated (Panel B) and CSCs-exposed (Panel C) groups relative to untreated controls (Panel A), while co-treatment with Nuciferine (Panels D and E) demonstrated significant attenuation of senescence markers in both models, indicating Nuciferine's potential protective effect against D-galactose- and CSCs-induced cellular aging.

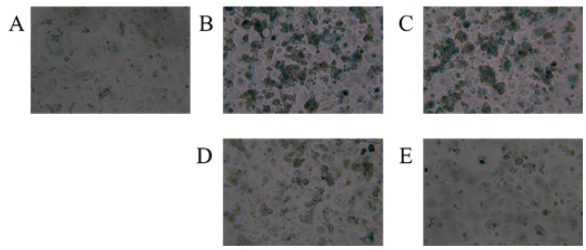

Fig. 4: Effect of Nuciferine on CSC-induced Cellular Senescence in HepG-2 Cells (β-galactosidase Staining, 200×): A: Normal control group B: D-galactose (D-gal) treatment group C: Cigarette smoke condensates (CSCs) treatment group D: Nuciferine + D-gal co-treatment group E: Nuciferine + CSC co-treatment group

NF Obviously Affected the Level of Indicators of Oxidative Damage in HepG-2 Cells Induced by CSCs

Figure 5 illustrates that relative to normal controls, D-galactose- and CSCs-induced senescence models manifested three distinct oxidative stress markers: significantly depressed SOD activity (P<0.05), markedly diminished GSH-Px content (P<0.05), and substantially elevated MDA accumulation (P<0.05). No statistically meaningful variation was detected between the two treatment groups (P>0.05). Nuciferine treatment demonstrated significant improvements in oxidative stress markers relative to model groups, elevating SOD and GSH-Px activities (P<0.05) while suppressing MDA generation (P<0.05). These findings collectively reveal Nuciferine's dual capacity to potentiate antioxidant enzyme function (SOD and GSH-Px) and attenuate lipid peroxidation (MDA) in HepG2 cells exposed to D-galactose- and CSCs-induced oxidative damage.

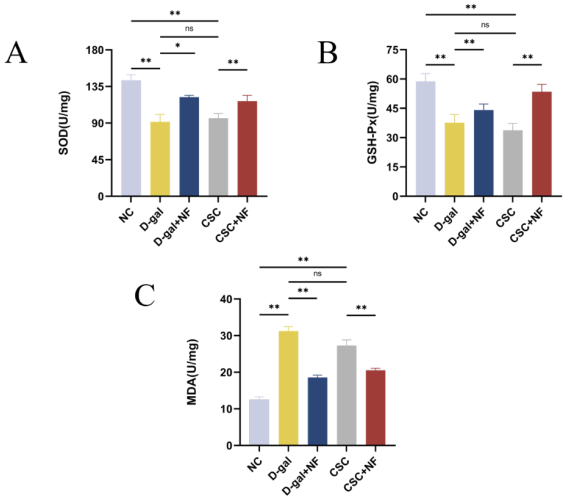

Fig. 5: HepG-2 cells biochemical indexes in different treatment groups. (A) The contents of SOD. (B) The contents of GSH-Px. (C) The contents of MDA. Results with P>0.05 were labeled as "ns" (not significant), those with P<0.05 with "*", and P < 0.01 with "**"

NF Obviously Ameliorated CSCs-Induced Senescence in HepG-2 Cells by Up-Regulating SIRT1 and Nrf2

To investigate the molecular mechanism of Nuciferine attenuating CSCs-induced senescence in HepG-2 cells, the expression levels of SIRT1, Nrf2, and FOXO1 genes were determined by qRT-PCR. The experimental results are shown in Figure 6. Experimental results demonstrated that both D-galactose and CSCs induction significantly downregulated the expression levels of these genes in HepG2 cells compared to the blank control group (P<0.05). However, Nuciferine intervention reversed these alterations, with significantly elevated expression of SIRT1, Nrf2, and FOXO1 observed in the Nuciferine-treated groups compared to their respective D-galactose and CSCs groups (P<0.05). These findings demonstrate that Nuciferine potentially exerts its anti-senescence effects on HepG2 cells by upregulating the gene expression of SIRT1, Nrf2, and FOXO1.

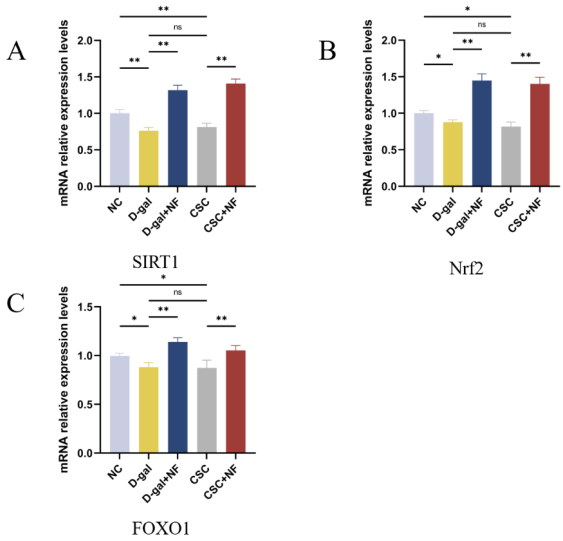

Fig. 6: The expression levels of mRNA in HepG-2 cells in different treatment groups. (A) Relative expression of SIRT1. (B) Relative expression of Nrf2. (C) Relative expression of FOXO1. Results with P>0.05 were labeled as "ns" (not significant), those with P<0.05 with "*", and P < 0.01 with "**"

NF Significantly Inhibited the Expression Level of miR-217-5p in CSCs-Induced HepG-2 Cells

To further investigate the mechanism underlying the interaction between Nuciferine and SIRT1, endogenous miRNA levels in HepG2 cells were analyzed. Both D-galactose and CSCs induction triggered a notable rise in miR-217-5p levels compared with untreated controls (P<0.05). However, Nuciferine intervention effectively downregulated miR-217-5p compared to D-galactose/CSCs-exposed cells (P<0.05).

Bioinformatic analysis (TargetScan + miRDB) identified putative binding regions of miR-217-5p on SIRT1 mRNA (Fig. 7C). Dual-luciferase reporter assays confirmed that hsa-miR-217-5p transfection with SIRT1-WT significantly reduced luciferase activity relative to the miR-NC control ($P<0.05$, Fig. 7B). This inhibitory effect was abolished when using mutated SIRT1 constructs ($P>0.05$), confirming a specific interaction between miR-217-5p and SIRT1 3′′-UTR.

These findings suggest that Nuciferine may upregulate SIRT1 expression in HepG2 cells through suppression of miR-217-5p, representing a potential post-transcriptional regulatory mechanism in cellular senescence.

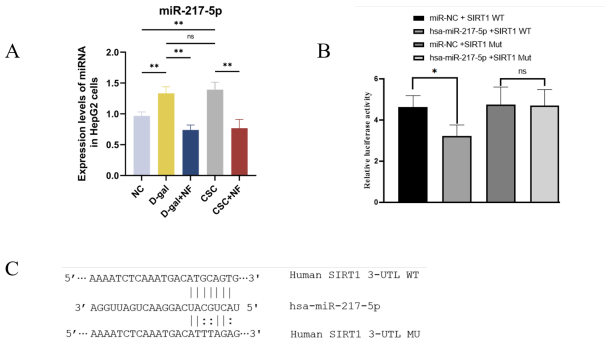

Fig. 7: The expression level of endogenous miRNA in HepG-2 cells and dual-luciferase reporter assay analysis. (A) miRNAs were extracted and the expression levels of miR-217-5p were detected by qRT-PCR. (B) the relative fluorescence values after transfection and mutation, which suggested that significant interaction existed between miR-217-5p and target gene SIRT1. (C) the binding site of miR-217-5p and corresponding target genes SIRT1. The dual-luciferase reporter assay confirmed that hsa-miR-217-5p binding to the wild-type SIRT1 3'-UTR significantly reduces luciferase activity (as shown by comparing the miR-NC + SIRT1 WT and hsa-miR-217-5p + SIRT1 WT groups in the figure). In contrast, when the complementary pairing is disrupted in the mutated SIRT1 3'-UTR, luciferase activity remains unchanged (as indicated by comparing the hsa-miR-217-5p + SIRT1 Mut and miR-NC + SIRT1 Mut groups)

Discussion

In recent years, there has been a growing recognition of the deleterious effects of smoking. This habit has been shown to impair both the structural and functional integrity of the liver, as evidenced by an increase in inflammatory responses and oxidative stress, and it may precipitate hepatocellular steatosis and fibrosis (Meng *et al.*, 2022; Xu *et al.*, 2025). Despite this, the precise mechanisms underlying smoking-induced hepatocellular damage and aging remain elusive, and there are no specific and effective treatments in clinical treatments. Prior research (Ge *et al.*, 2022) characterized the composition of Cigarette Smoke Components (CSCs), identifying Nicotine, Phenol, 2,4-bis(1,1-dimethylethyl) phenol, and Triacetin as the principal constituents, aligning with existing literature. Consequently, the investigation of natural products capable of mitigating and counteracting smoking-induced hepatocellular senescence holds significant promise for clinical applications.

The lotus leaf, a natural botanical, possesses a myriad of pharmacological properties. Its main active ingredient, Nuciferine, also has pharmacological effects such as regulating lipid metabolism, lowering blood sugar, antioxidation, antibacterial, and antiviral effects (Wan *et al.*, 2022). Emerging research indicates that Nuciferine can alleviate oxidative damage to mammary epithelial cells caused by high non-esterified fatty acids (NEFA) by enhancing autophagy (Li *et al.*., 2023). Additionally, it has been demonstrated to ameliorate Non-Alcoholic Fatty Liver Disease (NAFLD) through the modulation of oxidative stress (Du *et al.*, 2022). In a recent experimental model, Nuciferine has been shown to significantly ameliorate HepG-2 cell aging induced by cigarette smoke components, reducing β-galactosidase expression levels and alleviating cellular senescence, findings that corroborate previous studies.

SIRT1, a deacetylase belonging to the Sirtuin family, is predominantly localized within the cellular nucleus. Studies have shown that SIRT1 regulates the level of oxidative stress by regulating multiple target genes and target proteins such as NF-κB, Nrf2, FOXO, etc., and plays an important role in physiological processes such as cell apoptosis and senescence (Chen *et al.*, 2020; Cui *et al.*, 2022). Nrf2 is a leucine zipper transcription factor that plays an important role in transcriptional regulation depending on the Antioxidant Response Element (ARE) (He *et al.*, 2020). This pathway transcriptionally regulates key antioxidant enzymes including SOD, CAT, and heme oxygenase, thereby alleviating oxidative damage (Yu & Xiao, 2021). FOXO1 can clear excess ROS by regulating downstream target genes such as Mn-superoxide dismutase (Mn-SOD), catalase. thereby reducing cell oxidative stress damage (Kyriazis *et al.*, 2021). SIRT1 is capable of activating Nrf2 and FOXO1, either directly or indirectly, to modulate the expression of antioxidant genes and thereby attenuate oxidative stress-induced cellular damage (Huang *et al.*, 2021).

Recent years scholarly work has demonstrated that SIRT1 can regulate the cell cycle protein B1 by deacetylating Nrf2, thereby ameliorateing oocyte aging (Ma *et al.*, 2018). Elevated expression levels of SIRT1 have been correlated with an extension in the lifespan of mice (Zhao *et al.*, 2021). Significantly, these observations align with the experimental results obtained in this study. Induction of CSCs leads to a significant decrease in the expression level of SIRT1 gene in HepG-2 cells, which can be significantly reversed by the intervention of NF. At the same time, NF intervention significantly increased the expression levels of Nrf2 and

FOXO1 genes in HepG-2 cells compared to CSCs-induced group ($P<0.05$). Correspondingly, the levels of SOD and GSH-Px in HepG-2 cells in NF intervention group were higher than those in CSCs group, and MDA expression level was lower than those in CSCs group, and these changes were significant ($P<0.05$). The above data indicated that NF was able to alleviate oxidative stress damage induced by CSCs in HepG-2 cells, and its mechanism may be that NF increase the expression of SIRT1 gene in HepG-2 cells, thereby up-regulating Nrf2 and FOXO1 target genes.

As a class of non-coding RNAs, miRNAs play crucial roles in numerous physiological activities. miRNA can interact with many cellular signaling pathways by inhibiting mRNA (Mohanapriya *et al.*, 2022; Turko *et al.*, 2025). Notably, studies have demonstrated that miR-217 induces senescence in vascular endothelial cells through its regulatory effect on the SIRT1/p53 pathway (Wang *et al.*, 2021). Additionally, the regulatory role of miR-217-5p in suppressing macrophage activation and redox imbalance induced by PM2.5 is mediated through STAT1 targeting, offering protective effects against PM2.5-associated pulmonary damage (Xie *et al.*, 2022). Collectively, these findings suggest that miR-217 is implicated in the regulation of oxidative stress and inflammatory responses. To further investigate how NF affects and regulates the expression level of the SIRT1 gene, an examination of endogenous miRNAs within HepG-2 cells was conducted. Quantitative analysis revealed a marked downregulation of miR-217 in the NF-treated group relative to CSCs-exposed cells ($P<0.05$). Dual-luciferase reporter assays validated the direct targeting relationship between miR-217 and SIRT1 mRNA, demonstrating miR-217-mediated suppression of SIRT1 expressionThese studies collectively indicate that NF may enhance the expression of the SIRT1 gene in HepG-2 cells affected by CSCs, potentially through the inhibition of miR-217-5p expression. While the dual-luciferase reporter assay provides valuable evidence for the potential interaction between miR-217-5p and SIRT1 3'UTR, this approach has inherent limitations. First, it relies on artificial reporter constructs rather than endogenous gene contexts, which may not fully recapitulate physiological regulatory mechanisms. Second, while it suggests targeting relationships, it does not demonstrate direct binding or functional consequences at the protein level. To comprehensively validate this regulatory axis, future studies should incorporate: (1) RNA immunoprecipitation (RIP) with anti-Ago2 antibodies to confirm miR-217-5p/SIRT1 mRNA incorporation into RISC complexes; (2) Western blot analysis to verify whether miR-217-5p overexpression or inhibition actually modulates SIRT1 protein expression; and (3) rescue experiments genetic and pharmacological approaches. These complementary methods would provide orthogonal evidence spanning molecular interaction, translational regulation, and functional relevance, substantially strengthening the mechanistic conclusions. We have explicitly noted this as an important direction for future investigation in our research framework.

Conclusion

In summary, The current research is at a fundamental stage, focusing on elucidating how NF counteracts Cigarette Smoke Component (CSC)-induced senescence in HepG-2 cells, with particular emphasis on the role of the miR-217/SIRT1/Nrf2 pathway in mediating NF's anti-senescence effects. At this phase, we aim to validate NF's intervention efficacy and its underlying cellular mechanisms. Through experimental approaches including cell viability assays (CCK-8), SA-β-galactosidase staining, oxidative stress marker measurements (SOD, GSH-Px, MDA), qRT-PCR, and dual-luciferase reporter assays, we have preliminarily demonstrated that NF alleviates cellular senescence by suppressing miR-217-5p expression and upregulating SIRT1, Nrf2, and FOXO1 gene expression levels. These findings provide critical insights into the potential anti-aging mechanisms of NF.

Future studies will address current limitations to further explore NF's anti-senescence mechanisms. Key directions involve investigating the reversibility of the miR-217/SIRT1/Nrf2 pathway through gene editing or pharmacological interventions to validate its therapeutic potential, extending research to in vivo models for evaluating NF's effects on systemic aging and related pathological changes, analyzing clinical samples to verify NF's efficacy and safety in humans, and assessing NF's impact across diverse cell types and senescence models to confirm the universality of findings. These investigations will establish a comprehensive and robust scientific foundation for developing NF-based therapeutic strategies against aging.

Acknowledgment

We would like to express our sincere gratitude to the National Natural Science Foundation of China, the Key Research & Development Program of Zhejiang Province and the Key Project of Science and Technology Plan of Zhejiang Provincial Market Supervision and Administration Bureau.

Funding Information

This work was supported financially by the National Natural Science Foundation of China (31100499 and 31672394), the Key Research & Development Program of Zhejiang Province (2024C03075), the Key Project of Science and Technology Plan of Zhejiang Provincial Market Supervision and Administration Bureau (ZD2025026).

Author's Contribution

Yun-Hong Zhao: Completed the experiments and wrote the manuscript.

Yi-Meng Ge, Wei-Jia Xu, Xue-Qing Wang: Completed parts of the experiments.

Jian Ge and Feng Guan: Designed and guided the experiments. Jian Ge analyzed the data and reviewed the manuscript.

Ethics

The authors declare that they have no conflict of interest.

References

Ahmad, A., Karim, A., Arfah, R. A., Agus, R., Ladju, R. B., Hidayah, N., Massi, M. N., Nurhasanah, A., Karim, H., Handayani, I., & Irfandi, R. (2024). Expression and Epitope Prediction of the Sirohydrochlorin Cobaltochelatase Isolated from a Local Strain of Mycobacterium Tuberculosis. *Emerging Science Journal*, *8*(4), 1345–1365. https://doi.org/10.28991/esj-2024-08-04-07

Chen, C., Zhou, M., Ge, Y., & Wang, X. (2020). SIRT1 and aging related signaling pathways. *Mechanisms of Ageing and Development*, *187*, 111215. https://doi.org/10.1016/j.mad.2020.111215

Cui, Z., Zhao, X., Amevor, F. K., Du, X., Wang, Y., Li, Diyan, Shu, G., Tian, Y., & Zhao, X. (2022). Therapeutic application of quercetin in aging-related diseases: SIRT1 as a potential mechanism. *Frontiers in Immunology*, *13*, 943321. https://doi.org/10.3389/fimmu.2022.943321

Dong, H., Zhao, Y., Teng, H., Jiang, T., Yue, Y., Zhang, S., Fan, L., Yan, M., & Shao, S. (2024). Pueraria lobata antioxidant extract ameliorates non-alcoholic fatty liver by altering hepatic fat accumulation and oxidative stress. *Journal of Ethnopharmacology*, *333*, 118468. https://doi.org/10.1016/j.jep.2024.118468

Du, X., Di Malta, C., Fang, Z., Shen, T., Niu, X., Chen, M., Jin, B., Yu, H., Lei, L., Gao, W., Song, Y., Wang, Z., Xu, C., Cao, Z., Liu, G., & Li, X. (2022). Nuciferine protects against high-fat diet-induced hepatic steatosis and insulin resistance via activating TFEB-mediated autophagy–lysosomal pathway. *Acta Pharmaceutica Sinica B*, *12*(6), 2869–2886. https://doi.org/10.1016/j.apsb.2021.12.012

Enc, F. Y., Ulasoglu, C., Bakir, A., & Yilmaz, Y. (2020). The interaction between current smoking and hemoglobin on the risk of advanced fibrosis in patients with biopsy-proven nonalcoholic fatty liver disease. *European Journal of Gastroenterology & Hepatology*, *32*(5), 597–600. https://doi.org/10.1097/meg.0000000000001536

Fang, Z., Jiang, X., Wang, S., Tai, W., Jiang, Q., Loor, J. J., Yu, H., Hao, X., Chen, M., Shao, Q., Song, Y., Lei, L., Liu, G., Du, X., & Li, X. (2024). Nuciferine protects bovine hepatocytes against free fatty acid–induced oxidative damage by activating the transcription factor EB/peroxisome proliferator-activated receptor γ coactivator 1 alpha pathway. *Journal of Dairy Science*, *107*(1), 625–640. https://doi.org/10.3168/jds.2022-22801

Ge, J., Xu, W., Chen, H., Dong, Z., Liu, W., Nian, F., & Liu, J. (2022). Induction mechanism of Cigarette Smoke Components (CSCs) on dyslipidemia and hepatic steatosis in rats. *Lipids in Health and Disease*, *21*(1), 117. https://doi.org/10.1186/s12944-022-01725-8

Granata, S., Canistro, D., Vivarelli, F., Morosini, C., Rullo, L., Mercatante, D., Rodriguez-Estrada, M. T., Baracca, A., Sgarbi, G., Solaini, G., Ghini, S., Fagiolino, I., Sangiorgi, S., & Paolini, M. (2023). Potential Harm of IQOS Smoke to Rat Liver. *International Journal of Molecular Sciences*, *24*(15), 12462. https://doi.org/10.3390/ijms241512462

He, F., Ru, X., & Wen, T. (2020). NRF2, a Transcription Factor for Stress Response and Beyond. *International Journal of Molecular Sciences*, *21*(13), 4777. https://doi.org/10.3390/ijms21134777

Huang, Y., Wang, S., Meng, X., Chen, N., & Li, S. (2021). Molecular Cloning and Characterization of Sirtuin 1 and Its Potential Regulation of Lipid Metabolism and Antioxidant Response in Largemouth Bass (Micropterus salmoides). *Frontiers in Physiology*, *12*, 726877. https://doi.org/10.3389/fphys.2021.726877

Kaur, G., Sundar, I. K., & Rahman, I. (2021). p16-3MR: A Novel Model to Study Cellular Senescence in Cigarette Smoke-Induced Lung Injuries. *International Journal of Molecular Sciences*, *22*(9), 4834. https://doi.org/10.3390/ijms22094834

Kyriazis, I. D., Hoffman, M., Gaignebet, L., Lucchese, A. M., Markopoulou, E., Palioura, D., Wang, C., Bannister, T. D., Christofidou-Solomidou, M., Oka, S., Sadoshima, J., Koch, W. J., Goldberg, I. J., Yang, V. W., Bialkowska, A. B., Kararigas, G., & Drosatos, K. (2021). KLF5 Is Induced by FOXO1 and Causes Oxidative Stress and Diabetic Cardiomyopathy. *Circulation Research*, *128*(3), 335–357. https://doi.org/10.1161/circresaha.120.316738

Li, J., Zhao, C., Liu, M., Chen, L., Zhu, Y., Gao, W., Du, X., Song, Y., Li, X., Liu, G., Lei, L., & Feng, H. (2023). Nuciferine Ameliorates Nonesterified Fatty Acid-Induced Bovine Mammary Epithelial Cell Lipid Accumulation, Apoptosis, and Impaired Migration via Activating LKB1/AMPK Signaling Pathway. *Journal of Agricultural and Food Chemistry*, *71*(1), 443–456. https://doi.org/10.1021/acs.jafc.2c06133

Liu, Q., Que, X., Yang, Y., Zhao, J., Tian, T., Wang, J., Fan, Z., Fang, H., & Song, Y. (2025). Study on the Enhancement of Hypoglycemic and Antioxidant Activities of Compound Herbal Tea through Solid-State Fermentation. *American Journal of Biochemistry and Biotechnology*, *21*(2), 129–140. https://doi.org/10.3844/ajbbsp.2025.129.140

Ma, R., Liang, W., Sun, Q., Qiu, X., Lin, Y., Ge, X., Jueraitetibaike, K., Xie, M., Zhou, J., Huang, X., Wang, Q., Chen, L., & Yao, B. (2018). Sirt1/Nrf2 pathway is involved in oocyte aging by regulating Cyclin B1. *Aging*, *10*(10), 2991–3004. https://doi.org/10.18632/aging.101609

Meng, L., Xu, M., Xing, Y., Chen, C., Jiang, J., & Xu, X. (2022). Effects of Cigarette Smoke Exposure on the Gut Microbiota and Liver Transcriptome in Mice Reveal Gut–Liver Interactions. *International Journal of Molecular Sciences*, *23*(19), 11008. https://doi.org/10.3390/ijms231911008

Menghini, R., Casagrande, V., Cardellini, M., Martelli, E., Terrinoni, A., Amati, F., Vasa-Nicotera, M., Ippoliti, A., Novelli, G., Melino, G., Lauro, R., & Federici, M. (2009). MicroRNA 217 Modulates Endothelial Cell Senescence via Silent Information Regulator 1. *Circulation*, *120*(15), 1524–1532. https://doi.org/10.1161/circulationaha.109.864629

Mohanapriya, R., Akshaya, R. L., & Selvamurugan, N. (2022). A regulatory role of circRNA-miRNA-mRNA network in osteoblast differentiation. *Biochimie*, *193*, 137–147. https://doi.org/10.1016/j.biochi.2021.11.001

Turko, R., Hajja, A., Magableh, A. M., Omer, M. H., Shafqat, A., Khan, M. I., & Yaqinuddin, A. (2025). The emerging role of miRNAs in biological aging and age-related diseases. *Non-Coding RNA Research*, *13*, 131–152. https://doi.org/10.1016/j.ncrna.2025.05.002

von Zglinicki, T. (2024). Oxidative stress and cell senescence as drivers of ageing: Chicken and egg. *Ageing Research Reviews*, *102*, 102558. https://doi.org/10.1016/j.arr.2024.102558

Wan, Y., Xia, J., Xu, J., Chen, L., Yang, Y., Wu, J.-J., Tang, F., Ao, H., & Peng, C. (2022). Nuciferine, an active ingredient derived from lotus leaf, lights up the way for the potential treatment of obesity and obesity-related diseases. *Pharmacological Research*, *175*, 106002. https://doi.org/10.1016/j.phrs.2021.106002

Wang, Z., Shi, D., Zhang, N., Yuan, T., & Tao, H. (2021). MiR-217 promotes endothelial cell senescence through the SIRT1/p53 signaling pathway. *Journal of Molecular Histology*, *52*(2), 257–267. https://doi.org/10.1007/s10735-020-09945-x

Wu, A.-G., Yong, Y.-Y., Pan, Y.-R., Zhang, L., Wu, J.-M., Zhang, Y., Tang, Y., Wei, J., Yu, L., Law, B. Y.-K., Yu, C.-L., Liu, J., Lan, C., Xu, R.-X., Zhou, X.-G., & Qin, D.-L. (2022). Targeting Nrf2-Mediated Oxidative Stress Response in Traumatic Brain Injury: Therapeutic Perspectives of Phytochemicals. *Oxidative Medicine and Cellular Longevity*, *2022*(1), 1015791. https://doi.org/10.1155/2022/1015791

Xie, J., Li, S., Ma, X., Li, R., Zhang, H., Li, J., & Yan, X. (2022). MiR-217-5p inhibits smog (PM2.5)-induced inflammation and oxidative stress response of mouse lung tissues and macrophages through targeting STAT1. *Aging*, *14*(16), 6796–6808. https://doi.org/10.18632/aging.204254

Xu, J., Li, Y., Feng, Z., & Chen, H. (2025). Cigarette Smoke Contributes to the Progression of MASLD: From the Molecular Mechanisms to Therapy. *Cells*, *14*(3), 221. https://doi.org/10.3390/cells14030221

Yang, X., Liu, Y., Cao, J., Wu, C., Tang, L., Bian, W., Chen, Y., Yu, L., Wu, Y., Li, S., Shen, Y., Xia, J., & Du, J. (2025). Targeting epigenetic and post-translational modifications of NRF2: key regulatory factors in disease treatment. *Cell Death Discovery*, *11*(1), 189. https://doi.org/10.1038/s41420-025-02491-z

Yang, Y. M., Cho, Y. E., & Hwang, S. (2022). Crosstalk between Oxidative Stress and Inflammatory Liver Injury in the Pathogenesis of Alcoholic Liver Disease. *International Journal of Molecular Sciences*, *23*(2), 774. https://doi.org/10.3390/ijms23020774

Yu, C., & Xiao, J.-H. (2021). The Keap1-Nrf2 System: A Mediator between Oxidative Stress and Aging. *Oxidative Medicine and Cellular Longevity*, *2021*(1), 6635460. https://doi.org/10.1155/2021/6635460

Zahara, E., Darmawi, Balqis, U., & Soraya, C. (2024). The Potential of Ethanol Extract of Aleurites Moluccanus Leaves as TNF-α Inhibitor in Oral Incision Wound Care Model. *Journal of Human, Earth, and Future*, *5*(4), 674–687. https://doi.org/10.28991/hef-2024-05-04-010

Zhang, Y., Yang, S., You, X., Li, Z., chen, L., Dai, R., Sun, H., & Zhang, L. (2025). Correction: CircSPG21 ameliorates oxidative stress-induced senescence in nucleus pulposus-derived mesenchymal stem cells and mitigates intervertebral disc degeneration through the miR-217/SIRT1 axis and mitophagy. *Stem Cell Research & Therapy*, *16*(1), 198. https://doi.org/10.1186/s13287-025-04337-y

Zhao, Y., Liu, X., Zheng, Y., Liu, W., & Ding, C. (2021). Aronia melanocarpa polysaccharide ameliorates inflammation and aging in mice by modulating the AMPK/SIRT1/NF-κB signaling pathway and gut microbiota. *Scientific Reports*, *11*(1), 20558. https://doi.org/10.1038/s41598-021-00071-6

Zulfikar, T., Siregar, T. N., Rozaliyani, A., & Sutriana, A. (2024). Antimicrobial Potential of Calotropis gigantea Leaf Against Klebsiella pneumoniae in Ventilator-Associated Pneumonia. *Journal of Human, Earth, and Future*, *5*(3), 456–470. https://doi.org/10.28991/hef-2024-05-03-010